Quantum Chemical and Kinetics Study of the Thermal Gas Phase Decomposition of 2-Chloropropene

ARTICLE *in* THE JOURNAL OF PHYSICAL CHEMISTRY A · SEPTEMBER 2013

Impact Factor: 2.69 · DOI: 10.1021/jp406931q · Source: PubMed

3 AUTHORS:

María Eugenia Tucceri
National Scientific and Technical Research Co…
27 PUBLICATIONS **221** CITATIONS
SEE PROFILE

María Badenes
National University of La Plata
20 PUBLICATIONS **122** CITATIONS
SEE PROFILE

Carlos J. Cobos
National Scientific and Technical Research Co…
126 PUBLICATIONS **3,054** CITATIONS
SEE PROFILE

THE JOURNAL OF PHYSICAL CHEMISTRY A

Article

pubs.acs.org/JPCA

Quantum Chemical and Kinetics Study of the Thermal Gas Phase Decomposition of 2-Chloropropene

María E. Tucceri,* María P. Badenes, and Carlos J. Cobos

Instituto de Investigaciones Fisicoquímicas Teóricas y Aplicadas (INIFTA), Departamento de Química, Facultad de Ciencias Exactas, Universidad Nacional de La Plata, Casilla de Correo 16, Sucursal 4, 1900 La Plata, Argentina

Supporting Information

ABSTRACT: A detailed theoretical study of the kinetics of the thermal decomposition of 2-chloropropene over the 600−1400 K temperature range has been done. The reaction takes place through the elimination of HCl with the concomitant formation of propyne or allene products. Relevant molecular properties of the reactant and transition states were calculated for each reaction channel at 14 levels of theory. From information provided by the BMK, MPWB1K, BB1K, M05-2X, and M06-2X functionals, specific for chemical kinetics studies, high-pressure limit rate coefficients of $(5.8 \pm 1.0) \times 10^{14}$ exp[−(67.8 ± 0.4 kcal mol^{-1})/RT] s^{-1} and $(1.1 \pm 0.2) \times 10^{14}$ exp[−(66.8 ± 0.5 kcal mol^{-1})/RT] s^{-1} were obtained for the propyne and allene channels, respectively. The pressure effect over the reaction was analyzed through the calculation of the low-pressure limit rate coefficients and falloff curves. An analysis of the branching ratio between the two channels as a function of pressure and temperature, based on these results and on computed specific rate coefficients, show that the propyne forming channel is predominant.

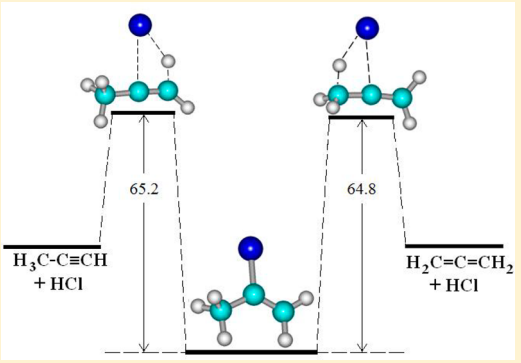

1. INTRODUCTION

Chlorinated compounds are important components of hazardous wastes, and certain chlorinated compounds are frequently found as products of incomplete combustion.[1] Because large amounts of these compounds are emitted into the atmosphere, it is highly necessary to investigate the degradation pathways, reaction rate coefficients, and product distributions to quantify their environmental impact.

Special attention have taken to gas phase reactions of hydrogen halide formation from thermal decomposition of alkyl halides, but there is limited information about similar reactions of unsaturated halides.[2] In particular, there are investigations for the HCl and HBr elimination from vinyl chloride[3,4] and vinyl bromide,[5] respectively. Also studies for the elimination of hydrogen chloride from 2-chloropropene[6−8] have been reported, where large discrepancies in the activation energies have been observed. In particular, Parsons et al.[6] made a theoretical study of the transition states leading to HCl elimination in order to assist in the interpretation of a photofragment translational spectroscopy study of 2-chloropropene.[9] The calculated barrier heights for the two distinct reaction channels, 1a and 1b, were respectively 72.5 and 73.2 kcal mol^{-1}, at the MP2/6-311G(d,p) level, 71.0 and 70.5 kcal mol^{-1} at the QCISD(T)/6-311+G(d,p)//MP2/6-311G(d,p) level, and 66.9 and 67.3 kcal mol^{-1} at the G3B3 level of theory.

$$CH_3CClCH_2 \rightarrow H_3C{-}C{\equiv}CH + HCl \quad (1a)$$

$$CH_3CClCH_2 \rightarrow H_2C{=}C{=}CH_2 + HCl \quad (1b)$$

On the other hand, Roy et al.[7] investigated the thermal decomposition of 2-chloropropene over the temperature range of 1100 to 1250 K and the Ar pressure range of about 1125 to 6000 Torr using single pulse shock tube experiments. They determined an activation energy of 67.9 ± 1.0 kcal mol^{-1} for the global dissociation process 1a + 1b and a ratio of 1.6 between the primary products of the reaction, propyne/allene. More recently, Nisar and Awan[8] reinvestigated the reaction at 668−747 K and at 11−76 Torr of pure 2-chloropropene in the presence of 1% of *n*-hexane as radical inhibitor in a conventional static system. A much smaller value of 58.0 ± 1.5 kcal mol^{-1} was derived for the activation energy, and propyne was the only olefinic product detected by chromatographic analysis. Despite the mentioned differences, in both studies, the 2-chloropropene follows first order kinetics decay, and only a small pressure effect has been observed in the first mentioned investigation. The activation energies determined by Roy et al. agree relatively well with those calculated by Parsons et al. but present differences of about 10 kcal mol^{-1} with the experimental values of Nisar and Awan. These discrepancies leads to differences of about 2−3 orders of magnitude in the rate coefficients over the 668−1250 K range.

To clarify the above discrepancies, a detailed kinetic study of the pressure and temperature dependencies of the 2-chloropropene thermal dissociation along their product

Received: July 13, 2013
Revised: September 12, 2013
Published: September 13, 2013

   dx.doi.org/10.1021/jp406931q | *J. Phys. Chem. A* 2013, 117, 10218−10227

Table 1. Structural Parameters of 2-Chloropropene Calculated at Different Levels of Theory (Bond Lengths in Angstroms and Angles in Degrees); the Experimental Data Are Also Included

parameter	exptl[a]	BMK	mPWB1K	BB1K	M05-2X	M06-2X
r(C−Cl)	1.744	1.763	1.727	1.729	1.742	1.744
r(−C−H)$_{avg}$	1.089	1.091	1.083	1.084	1.086	1.089
r(=C−H)$_{avg}$	1.089	1.081	1.074	1.075	1.077	1.080
r(C−C)	1.495	1.499	1.480	1.481	1.490	1.492
r(C=C)	1.338	1.324	1.314	1.315	1.319	1.321
∠(C=C−Cl)	119.0	119.8	120.0	119.9	119.9	119.9
∠(C−C−H$_{in\ plane}$)	112.1	110.0	110.3	110.3	110.0	110.2
∠(C−C−H$_{out\ of\ plane}$)	110.6	110.4	110.5	110.5	110.1	110.3
∠(C=C−H$_{trans\ to\ Cl}$)	118.7	119.3	119.5	119.5	119.4	119.4
∠(C=C−H$_{cis\ to\ Cl}$)	125.0	122.1	122.0	122.1	121.8	122.0
∠(C−C=C)	126.3	126.8	126.3	126.3	126.5	126.5

[a]Ref 29.

Table 2. Harmonic Vibrational Frequencies (in cm^{-1}), Approximate Assignments, and Infrared Intensities (in km mol^{-1}) Calculated at Different Levels of Theory for 2-Chloropropene; the Experimental and the Average of the Calculated Values Are Presented

approximate assignments	exptl[a]	BMK	mPWB1K	BB1K	M05-2X	M06-2X	average
stretching asym. CH_2	3121 (s)	3262 (0.2)	3327 (2)	3321 (2)	3306 (0.7)	3271 (0.5)	3297
stretching sym. CH_2	3025 (w)	3163 (0.7)	3229 (0.8)	3222 (0.8)	3211 (0.5)	3173 (0.7)	3200
stretching asym. CH_3	2992 (vs)	3142 (6)	3203 (11)	3196 (11)	3175 (8)	3149 (7)	3173
stretching asym. CH_3	2973 (vs)	3110 (3)	3176 (6)	3169 (6)	3156 (4)	3133 (3)	3149
stretching sym. CH_3	2940 (s)	3045 (6)	3107 (10)	3101 (11)	3091 (8)	3063 (8)	3081
stretching C=C	1645 (vs)	1712 (52)	1768 (54)	1763 (53)	1739 (52)	1728 (49)	1742
bending CH_3	1450 (s)	1512 (11)	1511 (11)	1509 (11)	1510 (12)	1495 (11)	1507
bending CH_3	1450 (s)	1496 (10)	1494 (11)	1492 (11)	1496 (11)	1482 (10)	1492
bending CH_2	1424 (m)	1451 (0.2)	1461 (1)	1458 (1)	1453 (1)	1441 (0.8)	1453
umbrella CH_3	1382 (s)	1417 (7)	1428 (9)	1426 (9)	1426 (10)	1413 (8)	1422
deformation	1184 (vs)	1220 (63)	1236 (61)	1232 (61)	1218 (59)	1210 (61)	1223
rocking CH_3	1046 (vw)	1082 (0)	1089 (0)	1087 (0)	1089 (0.1)	1081 (0)	1085
wagging CH_3	999 (w)	1022 (1)	1037 (1)	1034 (1)	1035 (0.9)	1029 (1)	1031
rocking CH_2	926 (s)	948 (5)	963 (4)	960 (4)	950 (4)	948 (4)	953
wagging CH_2	879 (vs)	941 (47)	950 (45)	946 (45)	949 (47)	947 (44)	946
wagging CH_2	692 (w)	730 (0)	734 (0.3)	732 (0.3)	729 (0.3)	733 (0.4)	731
stretching CCl	641 (vs)	671 (28)	678 (32)	675 (32)	643 (35)	655 (33)	664
C2 out of plane	434 (s)	453 (8)	465 (7)	464 (7)	450 (7)	458 (7)	458
bending CCC	396 (m)	406 (0.8)	406 (1)	405 (1)	405 (0.9)	409 (0.8)	406
bending ClCC	343 (m)	346 (0.9)	348 (0.9)	347 (0.9)	349 (1)	351 (1)	348
torsion C−CH_3	195 (vw)	242 (0.3)	215 (0.3)	215 (0.3)	211 (0.3)	242 (0.3)	225

[a]Ref 32.

branching ratio for reactions 1a and 1b, corresponding to the ratio of the reaction rate coefficient for the desired channel to the sum of the reaction rate coefficients for both channels, is presented in this work. To this purpose, the unimolecular rate theory complemented with molecular information provided by different quantum chemical methods were employed.

2. COMPUTATIONAL METHODS

Several formulations of the density functional theory (DFT) were used in this study. In particular, the popular hybrid functional B3LYP[10] and the more recent formulations B98,[11] O3LYP,[12] BMK,[13] MPWB1K,[14] BB1K,[15] M05-2X,[16] and M06-2X,[17] as implemented in the Gaussian09[18] program package, were employed. Also the long-range corrected functionals LC-wPBE,[19−22] wB97XD,[23] and CAM-B3LYP[24] were used. The large 6-311++G(3df,3pd) triple split valence basis set with diffuse and p, d, and f-type polarization functions included in the atoms was in all cases employed. At a higher level of theory, the ab initio CBS-QB3[25,26] and the G3B3 model chemistries[27] and the more recent, and accurate, implementation G4 were used.[28] Geometry optimizations without symmetry constraints were carried out using analytical gradient methods. At the calculated equilibrium structures, the harmonic vibrational frequencies were then derived via analytical second derivative methods. The synchronous transit-guided quasi-Newton (STQN) method was employed for locating transition structures.

3. RESULTS AND DISCUSSION

3.1. Molecular Structures and Harmonic Vibrational Frequencies. The geometrical parameters and harmonic vibrational frequencies for the 2-chloropropene and the transition states for reactions 1a and 1b were obtained using the aforementioned DFT and ab initio models. In particular, structural parameters and harmonic vibrational frequencies for 2-chloropropene calculated using the BMK, mPWB1K, BB1K,

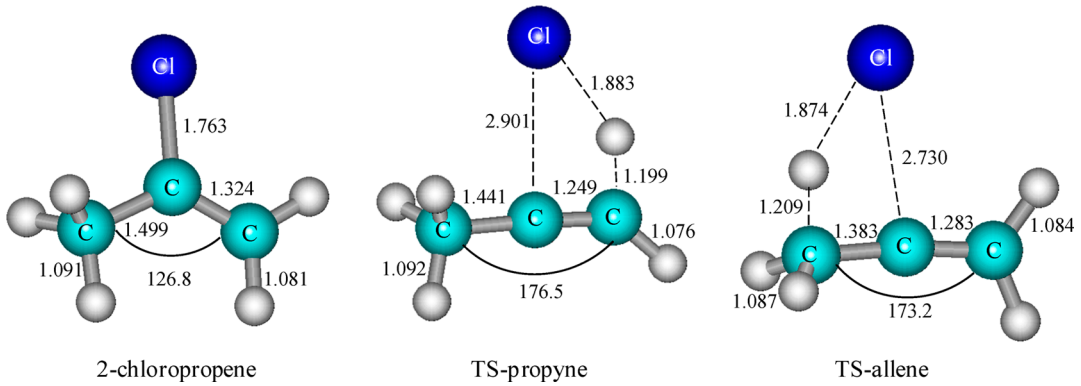

Figure 1. Geometrical structures of 2-cloropropene and its transition states obtained at BMK/6-311++G(3df,3pd) level of theory.

Table 3. Structural Parameters for the Two Transition States of the Decomposition of 2-Chloropropene Calculated at Different Levels of Theory (Bond Lengths in Angstroms and Angles in Degrees)

	TS-propyne					TS-allene				
parameters	BMK	mPWB1K	BB1K	M05-2X	M06-2X	BMK	mPWB1K	BB1K	M05-2X	M06-2X
r(C−Cl)	2.719	2.649	2.656	2.649	2.646	2.730	2.677	2.681	2.672	2.681
r(−C−H)$_{avg}$	1.089	1.081	1.082	1.087	1.086	1.088	1.079	1.080	1.082	1.085
r(−C−H)	1.099	1.091	1.092	1.094	1.096					
r(−C−HCl)						1.209	1.207	1.208	1.211	1.205
r(=C−H)	1.076	1.067	1.068	1.071	1.073	1.089	1.082	1.082	1.085	1.088
r(=C−HCl)	1.199	1.201	1.201	1.206	1.201	1.080	1.071	1.072	1.074	1.077
r(C−C)	1.441	1.427	1.428	1.438	1.439	1.383	1.368	1.368	1.378	1.380
r(C=C)	1.249	1.239	1.241	1.245	1.247	1.283	1.275	1.276	1.281	1.282
r(=CH−Cl)	1.883	1.846	1.849	1.867	1.880					
∠(C=C−Cl)	85.5	87.9	87.6	88.2	88.4	102.4	101.4	101.7	102.0	102.0
∠(C−C−H$_{in\ plane}$)	106.0	106.0	106.0	106.0	106.0	89.8	87.5	87.8	88.1	88.8
∠(C−C−H$_{out\ of\ plane}$)	110.6	110.8	110.9	110.5	110.4	115.5	116.2	116.2	115.9	115.7
∠(C=C−H$_{trans\ to\ Cl}$)	138.4	142.1	141.7	140.5	140.9	116.4	116.2	116.2	115.9	115.9
∠(C=C−H$_{cis\ to\ Cl}$)	94.1	90.3	90.7	91.2	91.5	123.1	123.2	123.3	123.1	123.4
∠(C−C=C)	176.5	175.7	175.5	175.0	175.0	173.2	172.8	172.7	171.7	172.2

M05-2X, and M06-2X functionals are presented in Tables 1 and 2, respectively. These DFT models, have been specifically developed for thermochemical kinetics studies and give mean absolute errors from experimental activation energies near 1 kcal mol^{-1}.[13−17] For this reason, they were especially selected for the present kinetics study. The results obtained with the other DFT and ab initio methods are listed in the Tables A and B of the Supporting Information.

The bond lengths and bond angles of 2-chloropropene calculated at each level of theory differ among themselves in only ±0.04 Å and ±0.8°, respectively. A good agreement was also found between the experimental[29] and calculated structural parameters where differences for the whole set of DFT models, close to ±0.02 Å and ±3.2° were observed. The resulting mean absolute deviations (MAD) are 0.006−0.015 Å and of about 1.4°. The BMK/6-311++G(3df,3pd) optimized structure is shown in the Figure 1. Previous reported values for the 2-chloropropene geometrical parameters at MP2/6-311G(d,p) and B3LYP/6-31G(d) levels from Parsons et al.,[6] B3LYP/6-311++G(3df,3pd) from Bae et al.,[30] and B3LYP/6-311++G(d,p) from Chang et al.[31] are in good agreement with the present results.

For the calculated harmonic vibrational frequencies of 2-chloropropene, differences up to 90 cm^{-1} were found among the whole group of density functional models and up to 65 cm^{-1} for the five models of Table 2. An inspection of Tables 2 and B of Supporting Information show also the very good correlation found between experimental[32] and calculated frequencies. In particular, MAD values between 59 and 80 cm^{-1} were obtained using the five functional selected for the kinetic study. All values are in good agreement with previous theoretical results.[6,30,31] In addition, mode assignments obtained from the animation of the normal modes and by comparison with species containing similar chemical groups, are included in Tables 2 and B (Supporting Information). Certainly, some of the modes are strongly coupled, and therefore, only approximate assignments are given.

Two structures for the transition state of reaction (1) were found at all employed levels of theory. TS-propyne corresponds to the four-center transition state to form HCl + propyne (channel 1a), and TS-allene corresponds to another four-center transition state to form HCl + allene (channel 1b). As it will be described in section 3.3.1, the TS-propyne is located at about 65 kcal mol^{-1} (including zero-point energies) over the 2-chloropropene ground state energy. The TS-allene is slightly more stable. The resultant geometries and vibrational frequencies for transition states calculated with the five functional here selected are listed in Tables 3 and 4, respectively. The corresponding results at the other levels of theory are presented in Tables C−E of the Supporting Information. The BMK/6-311++G(3df,3pd) optimized structures of both transition states are shown in the Figure 1. The

dx.doi.org/10.1021/jp406931q | J. Phys. Chem. A 2013, 117, 10218−10227

Table 4. Harmonic Vibrational Frequencies (in cm^{-1}), Approximate Assignments, and Infrared Intensities (in km mol^{-1}) Calculated at Different Levels of Theory for (a) the Transition State of Reaction 1a and (b) the Transition State of Reaction 1b

	(a) TS-propyne					
approximate assignments	BMK	mPWB1K	BB1K	M05-2X	M06-2X	average
stretching CH	3304 (87)	3388 (86)	3379 (82)	3363 (82)	3307 (90)	3348
stretching asym. CH_3	3167 (6)	3230 (4)	3224 (3)	3188 (5)	3163 (5)	3195
stretching asym. CH_3	3121 (3)	3184 (1)	3177 (1)	3145 (2)	3119 (2)	3149
stretching sym. CH_3	3017 (7)	3073 (5)	3065 (5)	3044 (5)	3017 (6)	3043
stretching C≡C	2003 (200)	2078 (202)	2070 (205)	2040 (200)	2040 (221)	2046
bending CCH	1814 (393)	1818 (464)	1817 (451)	1776 (412)	1798 (352)	1804
bending CH_3	1481 (6)	1487 (5)	1484 (5)	1491 (5)	1468 (4)	1482
bending CH_3	1446 (19)	1438 (20)	1436 (19)	1444 (20)	1422 (18)	1437
umbrella CH_3	1402 (9)	1401 (9)	1398 (9)	1422i (275)	1380 (8)	1397
rocking CH_2	1275i (257)	1260i (252)	1256i (238)	1405 (9)	1371i (141)	1317i
rocking CH_3	1070 (0.9)	1068 (0.9)	1066 (1)	1073 (1)	1054 (0.9)	1066
wagging CH_3	1026 (70)	1021 (16)	1020 (16)	1022 (49)	1007 (39)	1019
bending CH_2	976 (107)	996 (168)	996 (166)	972 (138)	977 (141)	983
wagging CH_2	869 (43)	864 (40)	865 (39)	857 (41)	856 (40)	862
bending CCH	838 (53)	857 (54)	857 (54)	840 (59)	832 (56)	845
wagging CH_2	565 (6)	580 (6)	578 (6)	567 (7)	569 (7)	572
bending CCC	503 (31)	495 (24)	497 (22)	493 (29)	476 (31)	493
C out of plane	331 (8)	343 (8)	343 (8)	337 (7)	335 (7)	338
stretching ClH	275 (143)	319 (162)	318 (157)	296 (171)	309 (172)	303
torsion C−CH_3	223 (0.1)	194 (0.2)	199 (0.3)	222 (0.2)	202 (0.2)	208
bending C≡CH	160 (28)	163 (22)	164 (22)	177 (26)	167 (27)	166
	(b) TS-allene					
approximate assignments	BMK	mPWB1K	BB1K	M05-2X	M06-2X	average
stretching CH	3271 (37)	3338 (32)	3331 (31)	3300 (32)	3257 (37)	3299
stretching asym. CH_3	3196 (6)	3263 (4)	3256 (3)	3236 (6)	3199 (6)	3230
stretching asym. CH_3 and CH_2	3128 (41)	3186 (30)	3179 (29)	3156 (32)	3120 (38)	3154
stretching sym. CH_3 and CH_2	3102 (14)	3167 (10)	3160 (10)	3143 (14)	3105 (14)	3135
stretching C=C	1971 (196)	2015 (170)	2009 (167)	1983 (162)	1983 (174)	1992
stretching CCl	1715 (549)	1693 (570)	1685 (557)	1655 (494)	1699 (516)	1689
bending CCH	1450 (3)	1463 (4)	1460 (4)	1463 (4)	1440 (3)	1455
bending CH_3 and CH_2	1354 (7)	1364 (7)	1363 (7)	1437i (363)	1347 (6)	1359
stretching CH	1295 (8)	1283 (7)	1281 (7)	1368 (7)	1329i (210)	1294i
stretching CH	1187i (265)	1257i (322)	1261i (314)	1277 (6)	1271 (7)	1281
stretching HCl	1167 (137)	1165 (149)	1163 (147)	1141 (145)	1155 (131)	1158
bending CCH	1055 (0)	1059 (0)	1056 (0)	1059 (0.1)	1044 (0.1)	1055
stretching CH	980 (48)	986 (20)	984 (20)	981 (37)	971 (36)	980
wagging CH_2	905 (48)	907 (66)	907 (64)	909 (66)	895 (68)	905
bending HCH	888 (57)	904 (51)	900 (51)	898 (54)	882 (52)	894
wagging CH_2	566 (1)	585 (2)	582 (2)	567 (2)	557 (2)	571
bending CCC	525 (35)	514 (34)	516 (33)	512 (41)	511 (36)	516
C out of plane	358 (6)	362 (6)	361 (6)	357 (6)	353 (6)	358
deformation	301 (166)	299 (177)	300 (171)	270 (158)	301 (181)	294
rocking CH_3	243 (3)	228 (3)	228 (3)	205 (53)	206 (24)	222
torsion C−CH_3	198 (26)	201 (22)	201 (23)	195 (2)	197 (2)	198

geometrical parameters for TS-propyne differ in about ±0.2 Å and ±10.5° among employed levels of theory (±0.07 Å and ±3.8° for the five density functional models of Table 3); whereas for TS-allene the differences are ±0.1 Å and ±6.4° (±0.06 Å and ±2.3° in Table 3). The highest differences were found in the C−Cl bond length and in the angles associated with that bond. Differences up to ±128 cm^{-1} (±84 cm^{-1} in Table 4a) and ±106 cm^{-1} (±67 cm^{-1} in Table 4b) were found for the vibrational frequencies of TS-propyne and TS-allene, respectively. The largest differences were found for the highest vibrational modes.

The transition state structures here calculated are similar to those reported by Parsons et al.[6] at the RHF/6-311G(d,p), MP2/6-311G(d,p), and B3LYP/6-31G(d) levels. More recently, Chang et al.[31] performed calculations to optimize structures of transitions states for the same reaction with the AM1-SRP and B3LYP/6-311++G(d,p) methods, finding a satisfactory agreement with the results derived by Parsons et al.[6] Our results, which were calculated with more recent DFT models and at a higher level of theory, are in reasonable agreement with the previous calculations.

3.2. Thermochemistry. In order to estimate the enthalpy changes for reactions 1a and 1b, the standard enthalpy of formation for 2-chloropropene was determined employing the following isodesmic and isogyric reactions

dx.doi.org/10.1021/jp406931q | J. Phys. Chem. A 2013, 117, 10218−10227

Table 5. Isodesmic Reaction Enthalpies and Enthalpies of Formation of 2-Cloropropene (in kcal mol^{-1})

	reaction 2		reaction 3		
level of theory	$\Delta H_{r,298}$	$\Delta H_{f,298}$	$\Delta H_{r,298}$	$\Delta H_{f,298}$	$\langle\Delta H_{f,298}\rangle$
BMK/6-311++G(3df,3pd)	−7.54	−4.46	−7.85	−4.32	−4.39
mPWB1K/6-311++G(3df,3pd)	−7.28	−4.20	−8.39	−4.86	−4.53
BB1K/6-311++G(3df,3pd)	−7.16	−4.08	−8.35	−4.82	−4.45
M05-2X/6-311++G(3df,3pd)	−7.66	−4.58	−7.94	−4.41	−4.50
M06-2X/6-311++G(3df,3pd)	−7.40	−4.32	−8.20	−4.67	−4.50
B3LYP/6-311++G(3df,3pd)	−6.60	−3.52	−7.62	−4.09	−3.81
G3B3	−7.90	−4.82	−8.56	−5.04	−4.93
G4	−7.95	−4.87	−8.66	−5.14	−5.01

$$CH_2CHCl + CH_3CH_3 \rightarrow CH_2CClCH_3 + CH_4 \quad (2)$$

$$CH_3CH_2Cl + CH_2CH_2 \rightarrow CH_2CClCH_3 + CH_4 \quad (3)$$

In such reactions, the number of each type of bonds in reactants and products as well as the spin multiplicities are conserved.[33] The computed enthalpy changes at 298 K, ΔH_r, and enthalpies of formation, $\Delta H_{f,298}$, for 2-chloropropene at different levels of theory are listed in Table 5.

To derive the $\Delta H_{f,298}$ values, the recommended experimental enthalpies of formation at 298 K (in kcal mol^{-1}) from Sander et al.[34] for CH_2CHCl (5.3 ± 0.7), CH_3CH_3 (−20.04 ± 0.07), CH_4 (−17.818 ± 0.014), CH_3CH_2Cl (−26.79 ± 0.47), and CH_2CH_2 (12.5 ± 0.1) were employed. Our results are in good agreement with the experimental value of −5.02 ± 2.2 kcal mol^{-1},[35] with that calculated by Thies Colegrove and Thompson of −5.4 kcal mol^{-1}[36] and with the value of −5.90 kcal mol^{-1} reported in the NIST evaluation[2] taken from the study of Shevtsova et al.[37] In particular, differences with the experimental value smaller than 0.09 kcal mol^{-1} were obtained with the G3B3 and G4 methods and about 0.5 kcal mol^{-1} with the BMK, mPWB1K, BB1K, M05-2X, and M06-2X methods. We recommend a $\Delta H_{f,298}$ value for 2-chloropropene obtained averaging the results at G3B3 and G4 of −5.0 kcal mol^{-1}. On the basis of the errors of experimental enthalpies and the dispersion of obtained values, a conservative error estimate of ±1.5 kcal mol^{-1} is assigned. Thus, the obtained value reduces the literature uncertainties. Table 6 shows the enthalpies of reactions 1a and 1b estimated using the standard enthalpy of formation derived here, together with those calculated in a direct way at different levels of theory. For HCl, $CHCCH_3$, and CH_2CCH_2, enthalpy of formation values of −22.06 ± 0.02, 44.2 ± 0.2, and 45.5 ± 0.3 kcal mol^{-1} were used.[34] As can be seen, both reactions are endothermic, reaction 1a in about 26.7 kcal mol^{-1} and 1b in about 28.0 kcal mol^{-1}. These results are in good agreement with those reported by Parsons et al.[6] If the value of −5.02 ± 2.2 kcal mol^{-1}[35] is used for the enthalpy of formation of 2-chloropropene, enthalpies of reaction of 27.2 and 28.5 kcal mol^{-1} for channels 1a and 1b, respectively, are obtained, in good agreement with our results.

Table 6. Enthalpy of Thermal Decomposition of 2-Chloropropene Calculated at Different Levels of Theory (in kcal mol^{-1})

	$CH_2{=}CClCH_3 \rightarrow CH{\equiv}CCH_3 + HCl$			$CH_2{=}CClCH_3 \rightarrow CH_2{=}C{=}CH_2 + HCl$		
		direct			direct	
level of theory	from isodesmic reactions at 298 K	0 K	298 K	from isodesmic reactions at 298 K	0 K	298 K
B3LYP	26.0	23.4	25.0	27.3	21.1	22.6
BMK	26.5	29.0	30.6	27.8	27.7	29.2
mPWB1K	26.7	28.3	29.8	28.0	27.6	29.0
BB1K	26.6	27.2	28.7	27.9	27.7	29.2
M05-2X	26.6	28.5	30.0	27.9	27.5	29.0
M06-2X	26.6	26.8	28.4	27.9	26.8	28.4
G3B3	27.1	25.5	27.0	28.4	26.5	27.9
G4	27.2	25.9	27.4	28.5	26.9	28.3

3.3. Theoretical Kinetics Analysis. *3.3.1. Electronic Transition State Barriers and High-Pressure Limit Rate Coefficients.* The electronic energy barriers between reactants and products for the channels 1a and 1b were estimated using the BMK, mPWB1K, BB1K, M05-2X, M06-2X, B3LYP, B98, O3LYP, LC-wPBE, wB97XD, and CAM-B3LYP density functional models with the extended 6-311++G(3df,3pd) basis set. As above-mentioned, the first five functionals provided results close to the chemical accuracy of about 1 kcal mol^{-1}.[13−17] In addition, the composite ab initio models CBS-QB3, G3B3, and G4 were also employed. A standard normal-mode-analysis indicates that all obtained transition state structures led to only one imaginary frequency indicating the presence of true transitions states. The computed electronic barriers at 0 K, $\Delta H^{\ddagger}_0$, for channels 1a and 1b at the five functionals here selected for the chemical kinetics calculations are listed in Table 7, and the results derived with the other quantum-chemical levels are presented in Table F of Supporting Information. The calculations predict four-center transition states located at 58−69 kcal mol^{-1} above the reactants. These results are in agreement with the barriers calculated by Parsons et al.[6] In particular, values of 65.2 ± 0.5 and 64.8 ± 0.4 kcal mol^{-1} were found for channels 1a and 1b, respectively, from the calculations with the five methods specific for thermochemical kinetics.

The high-pressure limit rate coefficient for this reaction, $k_{\infty 1}$, was calculated using the canonical formulation of the transition state theory. The vibrational and rotational partition functions were evaluated using the molecular input data obtained from the quantum-chemical calculations. To derive the Arrhenius parameters over the experimental range of the Roy et al.[7] and Nisar and Awan[8] investigations, high-pressure rate coefficients were calculated between 600 and 1400 K at each level of theory. The resulting high-pressure limit rate coefficients k_∞, pre-exponential factors A_∞ and activation energies $E_{a\infty}$ are listed in Tables 7 and F (Supporting Information). It should be noted that for the channel 1a similar results were obtained when the molecular partition functions were calculated assuming the CH_3 moiety in the 2-chloropropene and TS-propyne as a free rotor (moment of inertia of 3.110 amu Å^2[38,39] in the molecule and 3.2 amu Å^2 in TS-propyne) or a hindered

dx.doi.org/10.1021/jp406931q | J. Phys. Chem. A 2013, 117, 10218−10227

Table 7. Electronic Energy Barriers at 0 K, $\Delta H^{\ddagger}_0$ (in kcal mol^{-1}), High-Pressure Limit Rate Coefficients k_∞ (in s^{-1}), Pre-Exponential Factors A_∞ (in s^{-1}), and Activation Energies $E_{a\infty}$ (in kcal mol^{-1}) for Channels 1a and 1b of the Decomposition of 2-Chloropropene Calculated at Different Levels of Theory

	$CH_3{-}CCl{=}CH_2 \rightarrow$ [TS-propyne]$^{\ddagger} \rightarrow CH_3{-}C{\equiv}CH + HCl$							
	k_∞							
method	600 K	800 K	1000 K	1200 K	1400 K	A_∞	$E_{a\infty}$	$\Delta H^{\ddagger}_0$
M05-2X	8.5×10^{-11}	1.2×10^{-4}	6.4×10^{-1}	2.0×10^{2}	1.2×10^{4}	4.8×10^{14}	68.0	65.4
M06-2X	1.6×10^{-10}	2.1×10^{-4}	1.1×10^{0}	3.2×10^{2}	1.9×10^{4}	6.7×10^{14}	67.6	65.0
BMK	2.0×10^{-10}	2.5×10^{-4}	1.2×10^{0}	3.5×10^{2}	2.1×10^{4}	6.5×10^{14}	67.4	64.7
BB1K	1.1×10^{-10}	1.5×10^{-4}	7.8×10^{-1}	2.4×10^{2}	1.5×10^{4}	5.5×10^{14}	67.9	65.3
mPWB1K	7.9×10^{-11}	1.2×10^{-4}	6.6×10^{-1}	2.1×10^{2}	1.3×10^{4}	5.8×10^{14}	68.3	65.7
	$CH_3{-}CCl{=}CH_2 \rightarrow$ [TS-allene]$^{\ddagger} \rightarrow CH_2{=}C{=}CH_2 + HCl$							
	k_∞							
method	600 K	800 K	1000 K	1200 K	1400 K	A_∞	$E_{a\infty}$	$\Delta H^{\ddagger}_0$
M05-2X	5.4×10^{-11}	6.2×10^{-5}	2.8×10^{-1}	8.0×10^{1}	4.6×10^{3}	1.2×10^{14}	66.9	64.7
M06-2X	5.6×10^{-11}	6.5×10^{-5}	3.0×10^{-1}	8.6×10^{1}	5.0×10^{3}	1.4×10^{14}	67.0	64.9
BMK	7.5×10^{-11}	7.4×10^{-5}	3.1×10^{-1}	8.2×10^{1}	4.5×10^{3}	9.1×10^{13}	66.2	64.3
BB1K	5.6×10^{-11}	6.1×10^{-5}	2.7×10^{-1}	7.4×10^{1}	4.2×10^{3}	1.0×10^{14}	66.7	64.7
mPWB1K	3.7×10^{-11}	4.5×10^{-5}	2.1×10^{-1}	6.1×10^{1}	3.6×10^{3}	1.0×10^{14}	67.2	65.2

rotor (barrier height of 2.671 kcal mol^{-1}[39] in the molecule and 2.3 kcal mol^{-1} in TS-propyne). This is because the ratio between the partition functions of the transition state and the molecule is very close to 1 in both cases. However, for the channel 1b, TS-allene presents a rigid structure without internal rotation. For that reason, in our derivations, it was consider the torsional motion as a hindered rotation for the 2-chloropropene only for the channel 1b.

An inspection of Tables 7 and F (Supporting Information) shows that calculated activation energies are considerably higher than that measured by Nissar and Awan[8] of 58.0 ± 1.5 kcal mol^{-1}, and they are much closer to the one reported by Roy et al.[7] of 67.9 ± 1.0 kcal mol^{-1}. The average high-pressure limiting rate coefficients obtained for channels 1a and 1b over the 600−1400 K range with the BMK, MPWB1K, BB1K, M05-2X, and M06-2X functional are

$$k_\infty(1a) = (5.8 \pm 1.0) \times 10^{14} \exp[-(67.8 \pm 0.4 \text{ kcal mol}^{-1})/RT] \text{ s}^{-1} \quad (4)$$

$$k_\infty(1b) = (1.1 \pm 0.2) \times 10^{14} \exp[-(66.8 \pm 0.5 \text{ kcal mol}^{-1})/RT] \text{ s}^{-1} \quad (5)$$

The derived A_∞ values are similar to that reported by Roy et al.[7] of 6.3×10^{14} s^{-1}, but considerably larger than determined by Nissar and Awan[8] of 1.1×10^{13} s^{-1}. An Arrhenius plot of our and previous results is presented in Figure 2. It is clear that the present rate coefficients are in a good agreement with those reported by Roy et al.,[7] but pronounced differences with the data of Nissar and Awan[8] are evident.

An analysis of the branching ratio between the two channels based on these results and on computed specific rate coefficients is presented in section 3.3.4.

3.3.2. Limiting Low-Pressure Rate Coefficients. Although the experimental evidence indicates that the 2-chloropropene decomposition reaction is, under the studied conditions,[7,8] very close to the high-pressure first-order region, to confront with this finding a theoretical kinetics analysis over a wide total pressure range was carried out for both reaction channels. In the following, we will present values for the channel 1a, and those corresponding to the channel 1b will be indicated in brackets. At the low-pressure limit, the rate coefficient is proportional to the effective total pressure and can be conveniently represented by the product of the collision efficiency β_c and the strong-collision rate coefficient k_0^{SC}.[40] We have calculated the last factor using Troe's factorized formalism.[40] In this model, all the relevant terms contributing to k_0^{SC} are explicitly accounted for by specific factors

$$k_0 = \beta_c[M]Z_{LJ}(\rho_{vib,h}(E_0)kT/Q_{vib}) \exp(-E_0/kT) \times F_{anh}F_EF_{rot}F_{rotint} \quad (6)$$

All these factors were computed employing the average molecular parameters listed in Tables 1 to 4. Here, $\rho_{vib,h}(E_0) = 1.68 \times 10^{10}$ (kcal mol^{-1})$^{-1}$ (1.56×10^{10} (kcal mol^{-1})$^{-1}$) is the harmonic vibrational density of states of 2-chloropropene at the threshold dissociation energy $E_0 \approx \Delta H^{\ddagger}_0 = 65.2$ kcal mol^{-1} (64.8 kcal mol^{-1}) (see section 3.3.1), and $Q_{vib} = 11.5$ and 832.0 are the vibrational partition functions of 2-chloropropene calculated at 600 and 1200 K, respectively. The F factors take into account corrections for effects of anharmonicity F_{anh} =

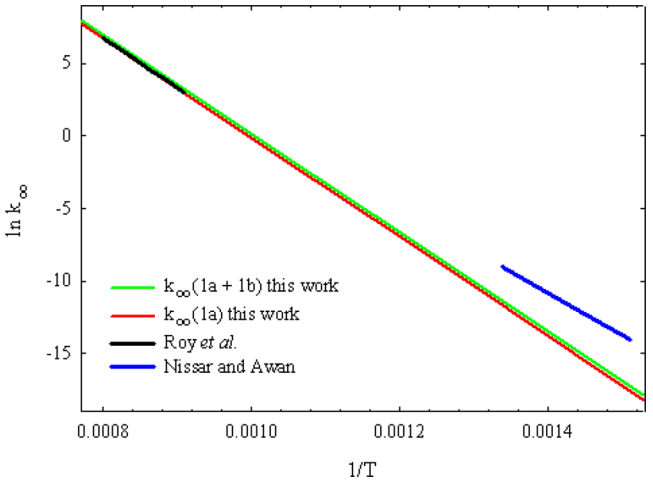

Figure 2. Arrhenius plot showing high-pressure limiting rate coefficients from this work and from previous investigations.

dx.doi.org/10.1021/jp406931q | J. Phys. Chem. A 2013, 117, 10218−10227

1.13, spread of internal energies F_E = 1.29 (1.29) and 1.77 (1.78) at 600 and 1200 K, external rotations F_{rot} = 2.68 (2.69) and 1.73 (1.73) at 600 and 1200 K (considering tight transition states), and internal rotations F_{rotint} = 3.66 (3.64) and 1.67 (1.66) at 600 and 1200 K. F_{rot} contributions were estimated using average rotational constants of 0.288, 0.117, and 0.084 cm^{-1} for TS-propyne (of 0.292, 0.114, and 0.084 cm^{-1} for TS-allene) and 0.314, 0.168, and 0.112 cm^{-1} for the 2-chloropropene. These parameters were derived from structural information provided by the BMK, mPWB1K, BB1K, M05-2X, and M06-2X calculations.

The calculation of Z_{LJ} requires the knowledge of the Lennard-Jones parameters σ and ε/k. We used, respectively, recommended values of 3.465 Å and 110.5 K for Ar,[41] and estimations (derived from molecular critical properties[37,41]) of 5.2 Å and 357.8 K for 2-chloropropene. The resulting collisional frequency values are $Z_{LJ} = 6.02 \times 10^{-10}$ cm^3 $molecule^{-1}$ s^{-1} (pure 2-chloropropene at 600 K) and 5.27×10^{-10} cm^3 $molecule^{-1}$ s^{-1} (highly diluted 2-chloropropene in Ar at 1200 K). Then, the strong collision low-pressure rate coefficients $k_0^{SC} = 2.7 \times 10^{-23}$[2-chloropropene] and $k_0^{SC} = 2.0 \times 10^{-13}$[Ar] cm^3 $molecule^{-1}$ s^{-1} were obtained for the channel 1a (and the values $k_0^{SC} = 3.5 \times 10^{-23}$[2-chloropropene] and $k_0^{SC} = 2.2 \times 10^{-13}$[Ar] cm^3 $molecule^{-1}$ s^{-1} for the channel 1b) at 600 and 1200 K, respectively. These rate coefficients were corrected by weak collision effects using reasonable β_c values of 0.4 for M = 2-chloropropene and 0.1 for M = Ar.[43] Finally, the resulting values for channel 1a are $k_0 = 1.1 \times 10^{-23}$ [2-chloropropene] (at 600 K) and $k_0 = 2.0 \times 10^{-14}$ [Ar] cm^3 $molecule^{-1}$ s^{-1} (at 1200 K), and $k_0 = 1.0 \times 10^{-23}$ [2-chloropropene] (at 600 K) and $k_0 = 2.2 \times 10^{-14}$ [Ar] cm^3 $molecule^{-1}$ s^{-1} (at 1200 K) for channel 1b. Provided the molecular input data are sufficiently well-known, a mean error value in the predicted k_0 values no better than a factor of 2 has been suggested.[40,43]

3.3.3. Falloff Behavior. The falloff behavior of dissociation and recombination reactions depends on specific parameters that characterize molecular collisions. In the present work, an analysis of the falloff curve with Troe's reduced method was performed.[43] This procedure employs the factorized expression[43]

$$k/k_\infty = F^{LH}(k_0/k_\infty)F(k_0/k_\infty) \quad (7)$$

The factor $F^{LH}(k_0/k_\infty) = (k_0/k_\infty)/(1 + k_0/k_\infty)$ is the result of the simple Lindemann–Hinshelwood mechanism. The broadening factor $F(k_0/k_\infty)$ accounts for corrections due to the energy and total angular momentum dependence of the excited species and for the multistep character of the energy transfer process assisted by collisions. This factor, at high temperatures, is represented by[44]

$$\log F(k_0/k_\infty) \approx \frac{\log F_{cent}}{1 + \left[\frac{\log(k_0/k_\infty) + c}{N - d(\log(k_0/k_\infty) + c)}\right]^2} \quad (8)$$

where $c = -0.4-0.67 \log F_{cent}$, $d = 0.14$, and $N \approx 0.75-1.27 \log F_{cent}$, and $F_{cent} = F(k_0/k_\infty = 1)$ is the center broadening factor. Here, F_{cent} is given by the product $F_{cent} \approx F^{WC}_{cent} F^{SC}_{cent}$, where F^{SC}_{cent} is the strong collision broadening factor[45]

$$-\log F^{SC}_{cent} = (1.06 \log S_T)^{2.2}/(1 + C_1 S_T^{C2}) \quad (9)$$

with

$$C_1 = 0.10 \exp(2.5B_T^{-1} - 0.22B_T - 6 \times 10^{-10}B_T^{6}) \quad (10)$$

$$C_2 = 1.9 + 4.6 \times 10^{-5}B_T^{2.8} \quad (11)$$

S_T and B_T are the Kassel parameters. The weak collision broadening factor F^{WC}_{cent} is related to the collision efficiency β_c by $\log F^{WC}_{cent} \cong 0.14 \log \beta_c$.[44]

To explore the pressure dependence of the unimolecular decomposition of 2-chloropropene, the falloff curve for the channel 1a was calculated. For this, the threshold barrier $\Delta H^{\ddagger}_0$ = 65.2 kcal mol^{-1} and the TS-propyne vibrational frequencies listed in Table 4a were employed. In this way, the calculated values are S_T = 6.65; B_T = 12.15 at 600 K and S_T = 10.51; B_T = 13.95 at 1200 K. As above, β_c values of 0.4 and 0.1 were employed, respectively, for the third-body 2-chloropropene at 600 K and for Ar at 1200 K.[42] Figure 3 shows the reduced

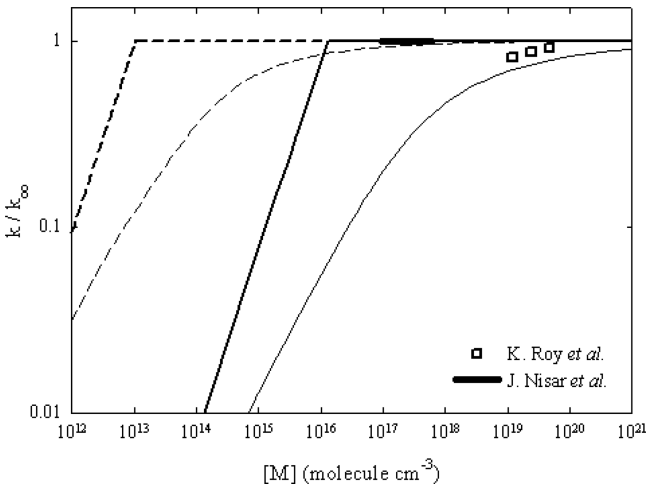

Figure 3. Reduced falloff curves for decomposition of 2-chloropropene at 600 K (dashed line) and at 1200 K (solid line) for the channel 1a. [M] = [2-chloropropene] at 600 K and [M] = [Ar] at 1200 K.

falloff curves obtained at the two studied temperatures for the reaction channel 1a. The same analysis was done for the channel 1b and a similar behavior was found for it but slightly shifted in the pressure axes (corresponding falloff curve is shown in Figure I of the Supporting Information).

The bath gas concentration corresponding to the center of the falloff curve, $[Ar]_c = k_\infty/k_0$, is indicated in Figure 3 by the intersection of the two straights lines. In this way, the values $[2\text{-chloropropene}]_c = 1.1 \times 10^{13}$ molecules cm^{-3} and $[Ar]_c = 1.3 \times 10^{16}$ molecules cm^{-3} are obtained at 600 and 1200 K, respectively ($[2\text{-chloropropene}]_c = 3.7 \times 10^{12}$ molecules cm^{-3} and $[Ar]_c = 3.5 \times 10^{15}$ molecules cm^{-3} for channel 1b). A comparison between the reported experimental data and the calculated falloff curves indicates that the lower temperature experiments of Nisar and Awan[8] are clearly very close to the high-pressure region of 2-chloropropene decomposition reaction. A small falloff behavior is apparent at the higher temperature. To comparison with the experimental data, we include in Figure 3 the rate coefficients obtained in the shock tube experiments of Roy et al. at 2, 4, and 8 bar and about 1200 K.[7] These values agree very well with ours, while the rate coefficient of 1.3×10^{-5} s^{-1},[8] derived in the temperature range of 660 and 750 K and pressure between 11 and 76 Torr using a conventional static system, is much higher than our value of 6.3

dx.doi.org/10.1021/jp406931q | J. Phys. Chem. A 2013, 117, 10218–10227

$\times 10^{-7}$ s^{-1} estimated for the same range of temperature and pressure.

3.3.4. Specific Rate Coefficients and Branching Ratio for the Two Reaction Channels. In order to estimate the branching ratio between the two possible channels of reaction 1, specific rate coefficients, $k(E,J)$, as a function of molecular total energy, E, and total angular momentum quantum number, J, have been calculated using RRKM theory[46]

$$k(E, J) = W(E, J)/h\rho(E, J) \quad (12)$$

Here $W(E,J)$ denotes the sum of rovibrational levels of the transition state, $\rho(E,J)$ the rovibrational density of states of the dissociating molecule, and h the Planck constant. For the sake of consistency, as before, all molecular input data employed in these calculations were obtained from an average of the results derived from the BMK, mPWB1K, BB1K, M05-2X, and M06-2X functionals combined with the 6-311++G(3df,3pd) basis set. Reduced moments of inertia for the C−CH_3 internal rotor of the molecule and TS-propyne were the same as in section 3.3.1. In these calculations $W(E,J)$ was evaluated by semi-classical state counting[47−49] and by direct state counting using the Beyer−Swinehart algorithm[50] with only slightly different results (see Figure II of Supporting Information). The K rotational quantum numbers for both the transition state and the molecule were considered active. On the other hand, as Figure II (Supporting Information) shows, anharmonicity corrections[51] were not significant. The resulting E- and J-resolved specific rate coefficients for both reaction channels are depicted in Figure 4.

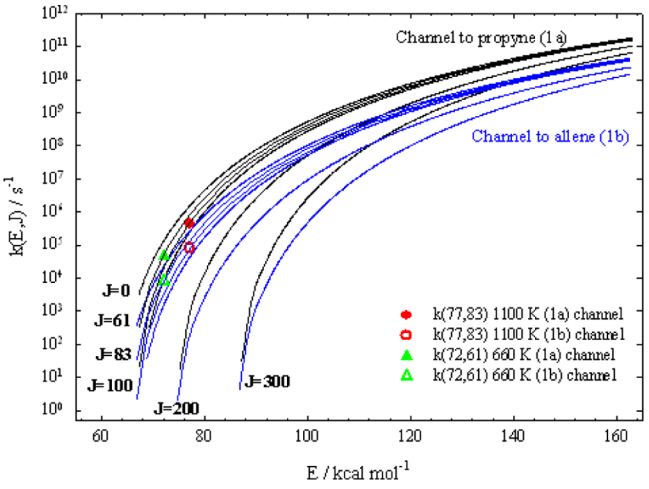

Figure 4. Specific rate coefficients, $k(E,J)$, as a function of total energy, E, and total angular momentum quantum number, J.

From the estimated average values E_T = 77 kcal mol^{-1} and J_T = 83, derived from a thermal distribution at 1100 K, the average values $k(E_T,J_T)$ = 4.5 × 10^5 s^{-1} for channel 1a and 7.7 × 10^4 s^{-1} for channel 1b were calculated. At 600 K, using the values E_T = 72 kcal mol^{-1} and J_T = 61, the average values of $k(E_T,J_T)$ of 4.6 × 10^4 s^{-1} for channel 1a and 7.9 × 10^3 s^{-1} for channel 1b were computed. These findings indicate that, over the studied temperature range, the branching ratio for the channel 1a is 0.86 at 1100 K and 0.85 at 600 K.

Energy resolved specific rate coefficients, $k(E)$, can be also easily estimated by using the inverse Laplace transform expression[52]

$$k(E) = A_\infty \rho(E - E_{a,\infty})/\rho(E) \quad (13)$$

which no requires information of the reaction transition state. This equation can be conveniently transformed to

$$k(E) = A_\infty [(E - E_{a,\infty} + a(E - E_{a,\infty})E_Z)/(E + a(E)E_Z)]^{s-1} \quad (14)$$

by using the Whitten−Rabinovitch approximation for the density of states.[49] Here, $a(E - E_{a,\infty})$ and $a(E)$ are correction factors to the zero-point vibrational energy E_Z of the dissociating molecule and s is the number of oscillators. Employing vibrational data of Table 2 and the Arrhenius parameters of eqs 4 and 5, the $k(E)$ values at different temperatures were calculated. The results at 600 K are 3.9 × 10^4 s^{-1} for channel 1a and 1.4 × 10^4 s^{-1} for channel 1b; however, at 1100 K, $k(E)$ of 8.2 × 10^5 s^{-1} for channel 1a and 2.4 × 10^5 s^{-1} for channel 1b were computed. These conduce to a branching ratio for the channel 1a of 0.77 at 1100 K and 0.74 at 600 K.

From all the kinetic results derived in the present work, it is possible to analyze the branching ratio for the channel 1a as a function of pressure. The branching in the high- and low-pressure limits were calculated from the rate coefficients derived in sections 3.3.1 and 3.3.2, and in the falloff region, it was estimated at an intermediate value of pressure from the results of section 3.3.3, as it is indicated in Table 8. The values

Table 8. Branching Ratio of the Channel 1a As a Function of Pressure; Intermediate Pressure Values Are [2-Chloropropene] = 5 × 10^{14} molecules cm^{-3} at 600 K and [Ar] = 2 × 10^{18} molecules cm^{-3} at 1200 K

pressure region	600 K	1200 K
low-pressure limit	0.52	0.48
intermediate pressure	0.63	0.74
high-pressure limit	0.70	0.78

listed in this Table show a clear dependence of the branching ratio in both temperature and pressure. These results indicate also that the thermal decomposition of 2-chloropropene proceeds mainly through the 1a channel at the high-pressure limit and in the falloff region. This is in very good agreement with the results reported by Parsons et al.[6] (branching for 1a channel of 0.78) and by Chang et al.,[31] and with the experimental observations of Roy et al.[7] (propyne to allene ratio of 1.6) and of Nissar and Awan[8] (propyne and HCl were the only products observed), in which the propyne formation channel is the predominant.

4. CONCLUSIONS

To clarify the differences of about 10 kcal mol^{-1} in the reported activation energies of the thermal decomposition of 2-chloropropene,[6−8] a theoretical study of the system between 600 and 1400 K was carried out. To this end, the unimolecular rate theory complemented with molecular information provided by DFT and high-level quantum chemical methods were employed.

The different calculations predict transition states located at about 58−69 kcal mol^{-1} above the reactant. These results are in good agreement with the electronic barriers calculated by Parsons et al.[6] In particular, by averaging the results obtained

dx.doi.org/10.1021/jp406931q | J. Phys. Chem. A 2013, 117, 10218−10227

using DFT methods developed for thermochemical kinetics, values of 65.2 ± 0.5 and 64.8 ± 0.4 mol^{-1} for $\Delta H^{\ddagger}_0$ were found for channels 1a and 1b, respectively. In addition, the high-pressure limit rate coefficients k_∞(1a) = (5.8 ± 1.0) × 10^{14} exp[−(67.8 ± 0.4 kcal mol^{-1})/RT] s^{-1} and k_∞(1b) = (1.1 ± 0.2) × 10^{14} exp[−(66.8 ± 0.5 kcal mol^{-1})/RT] were obtained. The resulting activation energies are considerably higher than that measured by Nissar and Awan[8] of 58.0 ± 1.5 kcal mol^{-1} and are in excellent agreement with the one reported by Roy et al.[7] of 67.9 ± 1.0 kcal mol^{-1}. A theoretical kinetics analysis over a wide pressure range shows that, according to the available experimental studies,[7,8] reaction 1 is very close to the high-pressure regime at the measured total pressures. However, the large discrepancies found between the kinetics data of both studies are not clear. Our results support the Roy et al. results.[7] From the computed rate coefficients, a somewhat larger predominance of reaction channel 1a is apparent.

■ ASSOCIATED CONTENT

Supporting Information

Part 1: Structural parameters and harmonic vibrational frequencies for the 2-chloropropene, TS-propyne, and TS-allene. Part 2: Electronic energy barriers at 0 K, high-pressure limit rate coefficients, pre-exponential factors, and activation energies for the decomposition of 2-chloropropene; reduced falloff curves for decomposition of 2-chloropropene for the channel 1b; and specific rate coefficients as a function of total energy and angular momentum quantum number. This material is available free of charge via the Internet at http://pubs.acs.org.

■ AUTHOR INFORMATION

Corresponding Author

*(M.E.T.) Tel: +54-221-4257430. Fax: +54-221-4254642. E-mail: mtucceri@inifta.unlp.edu.ar.

Notes

The authors declare no competing financial interest.

■ ACKNOWLEDGMENTS

This research project was supported by the Universidad Nacional de La Plata, the Consejo Nacional de Investigaciones Científicas y Técnicas (CONICET), and the Agencia Nacional de Promoción Científica y Tecnológica.

■ REFERENCES

(1) Tsang, W. Mechanisms for the Formation and Destruction of Chlorinated Organic Products of Incomplete Combustion. *Combust. Sci. Technol.* **1990**, *74*, 99−116.

(2) *NIST Chemical Kinetics Database Standard Reference Database 17*, Version 7.0 (Web Version), Release 1.6.3 Data Version 2011.06, 2011.

(3) Manion, J. A.; Louw, R. Gas-Phase Hydrogenolysis of Chloroethene: Rates, Products, and Computer Modelling. *J. Chem. Soc., Perkin Trans. 2* **1988**, *0*, 1547−1555.

(4) Zabel, F. Thermal Gas-Phase Decomposition of Chloroethylenes. II. Vinyl Chloride. *Int. J. Chem. Kinet.* **1977**, *9*, 651−662.

(5) Shilov, A. E.; Sabirova, R. D. The Mechanism of the Thermal Decomposition of Ethyl and Vinyl Iodides and the Simultaneous Occurrence of Two Types of Primary Decomposition of Alkyl Halides. *Kinet. Catal.* **1964**, *5*, 32−39.

(6) Parsons, B. F.; Butler, L. J.; Ruscic, B. Theoretical Investigation of the Transition States Leading to HCI Elimination in 2-Chloropropene. *Mol. Phys.* **2002**, *100*, 865−874.

(7) Roy, K.; Awan, I. A.; Manion, J. A.; Tsang, W. Thermal Decomposition of 2-Bromopropene and 2-Chloropropene. *Phys. Chem. Chem. Phys.* **2003**, *5*, 1806−1810.

(8) Nisar, J.; Awan, I. A. A Gas-Phase Kinetic Study on the Thermal Decomposition of 2-Chloropropene. *Kinet. Catal.* **2008**, *49*, 461−465.

(9) Mueller, J. A.; Parsons, B. F.; Butler, L. J.; Qi, F.; Sorkhabi, O.; Suits, A. G. Competing Isomeric Product Channels in the 193 nm Photodissociation of 2-Chloropropene and in the Unimolecular Dissociation of the 2-Propenyl Radical. *J. Chem. Phys.* **2001**, *114*, 4505−4521.

(10) Becke, A. D. Density Functional Thermochemistry. III. The Role of Exact Exchange. *J. Chem. Phys.* **1993**, *98*, 5648−5652.

(11) Schmider, H. L.; Becke, A. D. Optimized Density Functionals from the Extended G2 Test Set. *J. Chem. Phys.* **1998**, *108*, 9624−9631.

(12) Cohen, A. J.; Handy, N. C. Dynamic Correlation. *Mol. Phys.* **2001**, *99*, 607−615.

(13) Boese, A. D.; Martin, J. M. L. Development of Density Functionals for Thermochemical Kinetics. *J. Chem. Phys.* **2004**, *121*, 3405−3416.

(14) Zhao, Y.; Truhlar, D. G. Hybrid Meta Density Functional Theory Methods for Thermochemistry, Thermochemical Kinetics, and Noncovalent Interactions: The MPW1B95 and MPWB1K Models and Comparative Assessments for Hydrogen Bonding and van der Waals Interactions. *J. Phys. Chem. A* **2004**, *108*, 6908−6918.

(15) Zhao, Y.; Lynch, B. J.; Truhlar, D. G. Development and Assessment of a New Hybrid Density Functional Model for Thermochemical Kinetics. *J. Phys. Chem. A* **2004**, *108*, 2715−2719.

(16) Zhao, Y.; Schultz, N. E.; Truhlar, D. G. Design of Density Functionals by Combining the Method of Constraint Satisfaction with Parametrization for Thermochemistry, Thermochemical Kinetics, and Noncovalent Interactions. *J. Chem. Theory and Comput.* **2006**, *2*, 364−382.

(17) Zhao, Y.; Truhlar, D. G. The M06 Suite of Density Functionals for Main Group Thermochemistry, Thermochemical Kinetics, Noncovalent Interactions, Excited States, and Transition Elements: Two New Functionals and Systematic Testing of Four M06-Class Functionals and 12 Other Functionals. *Theor. Chem. Acc.* **2008**, *120*, 215−241.

(18) Frisch, M. J.; Trucks, G. W.; Schlegel, H. B.; Scuseria, G. E.; Robb, M. A.; Cheeseman, J. R.; Scalmani, G.; Barone, V.; Mennucci, B.; Petersson, G. A.; et al. *Gaussian 09*, revision A.02; Gaussian, Inc.: Wallingford, CT, 2009.

(19) Tawada, Y.; Tsuneda, T.; Yanagisawa, S.; Yanai, T.; Hirao, K. A Long-Range-Corrected Time-Dependent Density Functional Theory. *J. Chem. Phys.* **2004**, *120*, 8425−8433.

(20) Vydrov, O. A.; Scuseria, G. E. Assessment of a Long-Range Corrected Hybrid Functional. *J. Chem. Phys.* **2006**, *125*, 234109.

(21) Vydrov, O. A.; Heyd, J.; Krukau, A.; Scuseria, G. E. Importance of Short-Range Versus Long-Range Hartree-Fock Exchange for the Performance of Hybrid Density Functionals. *J. Chem. Phys.* **2006**, *125*, 074106.

(22) Vydrov, O. A.; Scuseria, G. E.; Perdew, J. P. Tests of Functionals for Systems with Fractional Electron Number. *J. Chem. Phys.* **2007**, *126*, 154109.

(23) Chai, J.-D.; Head-Gordon, M. Long-Range Corrected Hybrid Density Functionals with Damped Atom−Atom Dispersion Corrections. *Phys. Chem. Chem. Phys.* **2008**, *10*, 6615−6620.

(24) Yanai, Y.; Tew, D.; Handy, N. A New Hybrid Exchange−Correlation Functional Using the Coulomb-Attenuating Method (CAM-B3LYP). *Chem. Phys. Lett.* **2004**, *393*, 51−57.

(25) Montgomery, J. A., Jr.; Frisch, M. J.; Ochterski, J. W.; Petersson, G. A. A Complete Basis Set Model Chemistry. VI. Use of Density Functional Geometries and Frequencies. *J. Chem. Phys.* **1999**, *110*, 2822−2827.

(26) Montgomery, J. A., Jr.; Frisch, M. J.; Ochterski, J. W.; Petersson, G. A. A Complete Basis Set Model Chemistry. VII. Use of The Minimum Population Localization Method. *J. Chem. Phys.* **2000**, *112*, 6532−6542.

(27) Baboul, A. G.; Curtiss, L. A.; Redfern, P. C.; Raghavachari, K. J. Gaussian-3 Theory Using Density Functional Geometries and Zero-Point Energies. *Chem. Phys.* **1999**, *110*, 7650−7657.

(28) Curtiss, L. A.; Redfern, P. C.; Raghavachari, K. Gaussian-4 Theory. *J. Chem. Phys.* **2007**, *126*, 084108.
(29) Hilderbrandt, R. L.; Schei, S. H. 2-Chloropropane and 2-Bromopropane: Gas-Phase Molecular Structures as Determined by Combined Analysis of Electron Diffraction and Microwave Spectroscopic Data. *J. Mol. Struct.* **1984**, *118*, 11−20.
(30) Bae, Y. J.; Lee, M.; Kim, M. S. One-Photon Mass-Analyzed Threshold Ionization Spectroscopy of 2-Chloropropene (2-C_3H_5Cl) and Its Vibrational Assignment Based on The Density-Functional Theory Calculations. *J. Chem. Phys.* **2005**, *123*, 044306.
(31) Chang, C.; Huang, Y.; Liu, S.; Lee, Y.; Pombar-Pérez, M.; Martínez-Nuñez, E.; Vázquez, S. A. Internal Energy of HCl Upon Photolysis of 2-Chloropropene at 193 nm Investigated With Time-Resolved Fourier-Transform Spectroscopy and Quasiclassical Trajectories. *J. Chem. Phys.* **2008**, *129*, 224301−11.
(32) Hunziker, H.; Günthard, H. H. Vibrational Spectra of Eight Isotopic Species, Valence Force Constants and Rotational Barrier of 2-Chloropropene. *Spectrochim. Acta* **1965**, *21*, 51−76.
(33) Hehre, W. J.; Radom, L.; Schleyer, P. v. R.; Pople, J. A. *Ab Initio Molecular Orbital Theory*; Wiley: New York, 1986.
(34) Sander, S. P.; Friedl, R. R.; Barker, J. R.; Golden, D. M.; Kurylo, M. J.; Wine, P. H.; Abbatt, J. P. D.; Burkholder, J. B.; Kolb, C. E.; Moortgat, G. K.; Huie, R. E.; Orkin, V. L. Chemical Kinetics and Photochemical Data for Use in Atmospheric Studies, NASA/JPL Data Evaluation, JPL Publication 06-2 Evaluation No. 17, NASA, Pasadena, CA, June 1, 2011; http://jpldataeval.jpl.nasa.gov/.
(35) Pedley, J. B.; Naylor, R. D.; Kirby, S. P. *Thermochemical Data of Organic Compounds*; 2nd ed.; Chapman and Hall: New York, 1986.
(36) Thies Colegrove, B.; Thompson, T. B. Ab Initio Heats of Formation for Chlorinated Hydrocarbons: Allyl Chloride, *cis*- and *trans*-1-Chloropropene, and Vinyl Chloride. *J. Chem. Phys.* **1997**, *106*, 1480−1490.
(37) Shevtsova, L. A.; Rozhnov, A. M.; Andreevskii, D. N. Equilibrium Dehydrochlorination of 2,2-Dichloropropane. *Russ. J. Phys. Chem.* **1970**, *44*, 852−855.
(38) Bell, S.; Guirgis, G. A.; Fanning, A. R.; Durig, J. R. Torsional Transitions and Barriers to Internal Rotation of the 2-Halopropenes. *J. Mol. Struct.* **1988**, *178*, 63−78.
(39) Unland, M. L.; Weis, V.; Flygare, W. H. Barrier Studies in the Halopropenes. I. The Microwave Spectrum, Barrier to Internal Rotation, Quadrupole Coupling Constants, and Microwave Double-Resonance Spectra of 2-Chloropropene. *J. Chem. Phys.* **1965**, *42*, 2138−2149.
(40) Troe, J. Theory of Thermal Unimolecular Reactions at Low Pressures. II. Strong Collision Rate Constants. Applications. *J. Chem. Phys.* **1977**, *66*, 4758−4775.
(41) Poling, B. E.; Prausnitz, J. M.; O'Connell, J. P. *The Properties of Gases and Liquids*, 5th ed.; McGraw-Hill: New York, 2001.
(42) Mourits, F. M.; Rummens, F. H. A. A Critical Evaluation of Lennard−Jones and Stockmayer Potential Parameters and of Some Correlation Methods. *Can. J. Chem.* **1977**, *55*, 3007−3020.
(43) Troe, J. Predictive Possibilities of Unimolecular Rate Theory. *J. Phys. Chem.* **1979**, *83*, 114−126.
(44) Gilbert, R. G.; Luther, K.; Troe, J. Theory of Thermal Unimolecular Reactions in the Fall-Off Range. II. Weak Collision Rate Constants. *Ber. Bunsenges. Phys. Chem.* **1983**, *87*, 169−177.
(45) Troe, J. Theory of Thermal Unimolecular Reactions in the Fall-Off Range. I. Strong Collision Rate Constants. *Ber. Bunsenges. Phys. Chem.* **1983**, *87*, 161−169.
(46) Zhu, L.; Hase, W. L. *A General RRKM Program QCPE 644*; Indiana University: Bloomington, IN.
(47) Tardy, D. C.; Rabinovitch, B. S.; Whitten, G. Z. Vibration-Rotation Energy-Level Density Calculations. *J. Chem. Phys.* **1968**, *48*, 1427−1429.
(48) Whitten, G. Z.; Rabinovitch, B. S. Approximation for Rotation-Vibration Energy Level Sums. *J. Chem. Phys.* **1964**, *41*, 1883−1883.
(49) Whitten, G. Z.; Rabinovitch, B. S. Accurate and Facile Approximation for Vibrational Energy-Level Sums. *J. Chem. Phys.* **1963**, *38*, 2466−2473.
(50) Beyer, T.; Swinehart, E. F. Number of Multiply-Restricted Partitions [A1]. *Commun. ACM* **1973**, *16*, 379−379.
(51) Haarhoff, P. C. The Density of Vibrational Energy Levels of Polyatomic Molecules. *Mol. Phys.* **1963**, *7*, 101−117.
(52) Forst, W. Unimolecular Rate Theory Test in Thermal Reactions. *J. Phys. Chem.* **1972**, *76*, 342−348.